24th COBEM - 2017

24th ABCM International Congress of Mechanical Engineering
December 3-8, 2017, Curitiba, PR, Brazil

COBEM-2017-1679
EXPERIMENTAL SET-UP FOR LOST CIRCULATION CONTROL IN FRACTURED CHANNEL BY PARTICULATE FLOW

Cássio Luís Schneider
Fernando César De Lai
Silvio Luiz de Mello Junqueira
Research Center for Rheology and Non-Newtonian Fluids (CERNN), Graduate Program in Mechanical and Materials Engineering (PPGEM), Federal University of Technology – Paraná (UTFPR), Curitiba, Brazil.
cassioschneider@alunos.utfpr.edu.br, fernandodelai@utfpr.edu.br, silvio@utfpr.edu.br

Abstract. *In this work the lost circulation phenomenon and the process of filling fractures through the injection of solid particles into a flow are investigated experimentally. The experimental set-up comprises a rectangular test section with a transverse fracture, instrumented with pressure gauges, flow and temperature monitors. In order to characterize the fracture filling pattern, the influence of variations of the particle type and concentration, the fracture outlet initial flow rate, the Reynolds number and the fracture thickness along the position, length and height of the formed bed of particles are investigated. The particulate flow is represented by a solution of water-glycerin with solid particles, abrasive plastic and glass spheres are used. Results show that all the parameters present the ability to modify the geometric characteristics of the bed, having a direct influence on the filling time and the fluid lost by the fracture.*

Keywords: *liquid-solid flow, lost circulation, fractured channel, experimental set.*

1. INTRODUCTION

The high costs and the increasing complexity of processes associated with the oil exploration and production have required numerous studies focusing on problems concerning the well drilling. The solutions found in these studies seek to minimize the use of remedial jobs and the non-productive time (NPT) during drilling (Kumar and Savari, 2011).

The drilling is performed by the rotational movement of a drill that compresses and grinds the rock, generating a lot of gravels. The outcoming cuttings are removed continuously due to the drilling fluids which is injected into the drill column and returns to the surface through the annulus region between the substrate walls and the drilling column (Azar and Samuel, 2007).

The drilling may damage the wall and the rock formation that surrounds it. Such damage, that appears in the form of cracks and fractures, is due to the high pressure gradients associated to the process, which facilitates the fluid invasion towards the formation as the porous substrate gets fractured. Therefore, a phenomenon rather indesirable for the oil industry, so called lost circulation, takes place. The lost circulation is defined as the drilling fluid that flows towards the rock formation through the pores or cracks in the well-formation set, which is aggravated since a preferential flow is verified if the formation is fractured (Cook *et al*., 2012; Almagro *et al*., 2014). Among all the different ways to control such phenomenon, the process of injecting solid particles with the drilling fluid to seal the fractures has been the focus of plenty of studies in the last decade. Such method consists of adding particulate material with selected granulometry, namely Lost Circulation Materials (LCM), to the drilling fluid (Whitfill and Hemphill, 2004; Suyan *et al*., 2007).

The objective of this work is to analyze experimentally, considering a vertical channel with a transversal fracture, the addition of particulate material to the fluid injection process in order to fill the fracture through the particles deposition. Results show the influence of variations of the particle type and concentration, the fracture thickness, flow rate at the fracture end and the Reynolds number over the fracture filling process. For that, parameters such as the length, the final height and the starting position of the formed bed and also the time to observe partial or total sealing of the fracture are monitored.

2. PROBLEM FORMULATION

Operations in the oil and gas industry have a high complexity of parameters commonly associated to geometry and operating conditions. In order to make the analysis possible some assumptions, presented in Fig. 1(a), must to be done.

A vertical channel (representing the oil well) with a single fracture in a horizontal plane is considered; the geometry is symmetrical about the center of the drill column. As displayed in Fig. 1(b), the fluid flow inside the column is not the focus of this work, as the goal is to observe the particle transport in the annulus and the particle deposition inside the fracture. Moreover, such assumption refers to the formation adjacent to the well, which is considered as impermeable.

The Figure 1(c) shows the region of interest for the study, in which the fracture is represented by its length, h_{FR}, and thickness, e_{FR}. With regards to the vertical channel, the length upstream and downstream the fracture are represented by l_{UP} and l_{DW}, respectively. Therefore the fluid loss control occurs as the particulate material is injected with the drilling fluid, in order to obtain the fracture filling along the time.

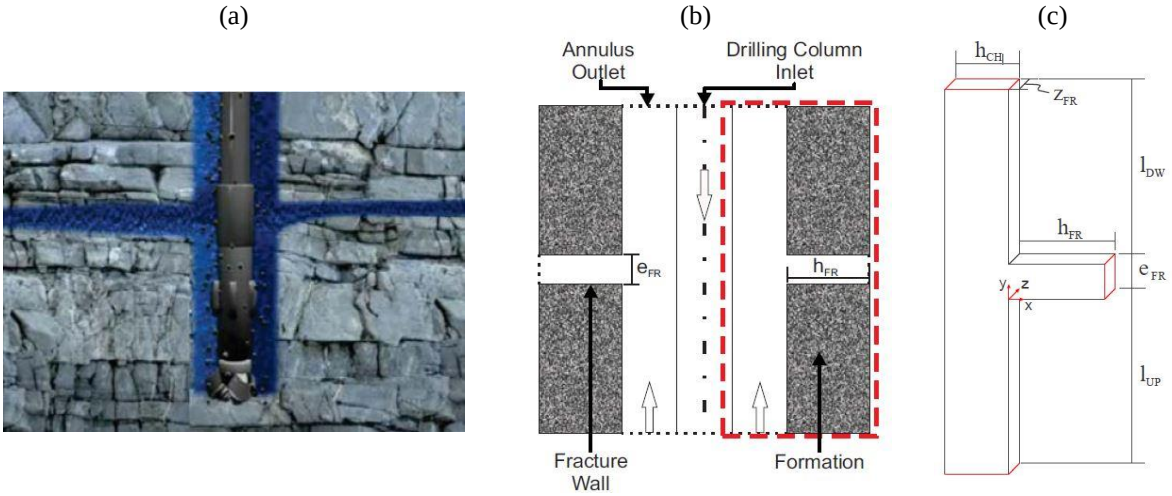

Figure 1. Simplifications: (a) well-fracture set; (b) idealization and (c) region of interest.
(Adapted from Barbosa *et al*., 2016)

3. EXPERIMENTAL PROCEDURE

The tests were performed in an experimental set designed and built to characterize the particle flow and the bed of particles formation along the fracture. Figure 2(a) shows the hydraulic circuit diagram and Fig. 2(b) shows the key components of the experimental set installed on the Porous Media Lab dependencies (LaMP) at the Research Center for Rheology and Non-Newtonian Fluids (CERNN – UTFPR).

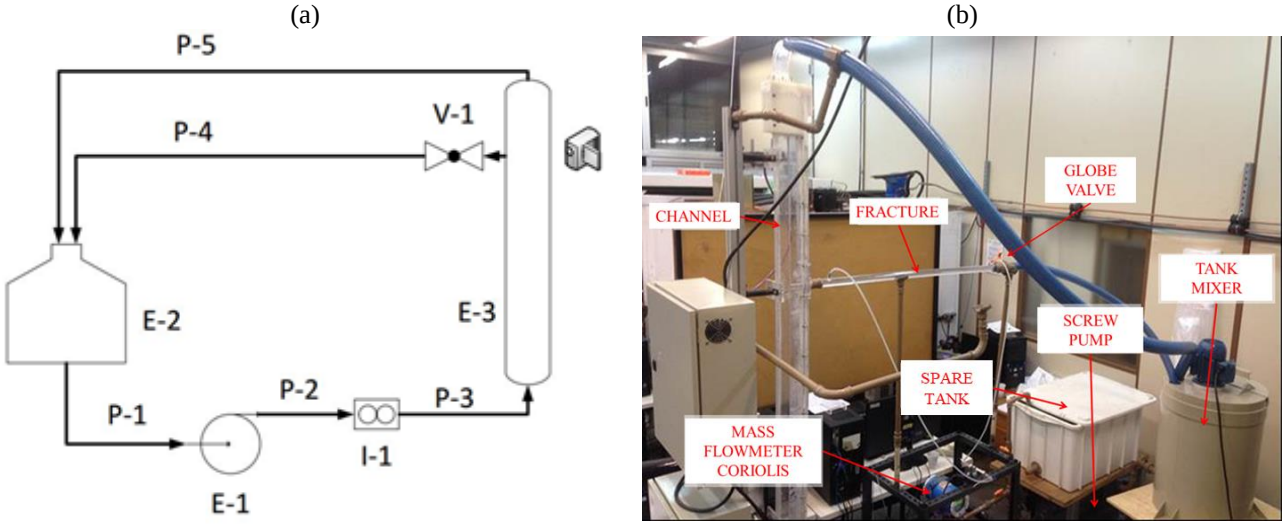

Figure 2. Experimental set: (a) hydraulic circuit diagram and (b) overview of the key components.

The experimental set consists of a tank with mixer (E-2) to homogenize the liquid-solid solution, in which there is a J type thermocouple to measure the solution temperature during the tests. A screw pump (E-1) provides the flow through the entire circuit. After leaving the pump the solution passes through a Coriolis type mass flowmeter (I-1) designed to measure the mass flow rate in real time before reaching the test section (E-3). The test section present two

exits (one at the upper nozzle and another at the end of the fracture); the fluid is redirected to the tank via two hoses (P-4 and P-5) which have larger diameters than the outlets, so that the pressures are atmospheric (Schneider *et al*., 2017).

The test section is made of acrylic to allow the capturing not only of the flow images but also the particles bed formed along the fracture. The test section, designed to represent the well annulus region, has a rectangular cross section of 45x16mm and 2m long. The fracture is located 1.28m from the vertical channel inlet to ensure a fully developed flow. The channel width represents the dimension of the annular region, for a well opening with outer and inner diameter, of 8.5 and 5 inches, respectively. Such dimensions are based on a given step of the drilling process, as suggested by De Lai *et al*. (2015) and Calçada *et al*. (2015). In order to measure the local pressure, the section has two relative pressure transducers: one (I-3) located 0.23m from the channel inlet and the other (I-2) located near the channel outlet (1.77m) above the fracture. Figure 3 shows the transmitters position and the test section dimensions.

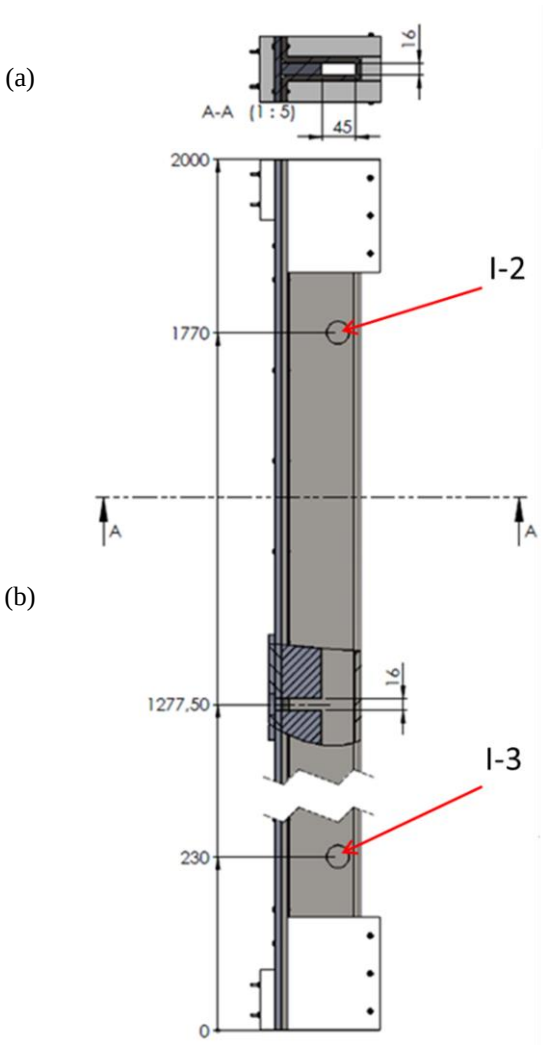

Figure 3. Test section representation: (a) cross section and (b) lateral view.

A solution containing 68.9% of glycerin mass concentration in water, with a density (ρ_g) at 25ºC of 1.17g/cm³ and dynamic viscosity (μ_g) of 16.912×10^{-3} Pa.s at 25ºC, was used during the tests. Particles of abrasive plastic (urea) and glass spheres, displayed in Fig. 4, with density of 1.50g/cm³ and 2.50g/cm³, respectively, were added to the solution to obtain different mass concentrations of particulate material (C_p).The resulting fluid to particulate mass ratio ($\rho_{p/g}$) is about 1.28 for the urea and 2.14 for the glass spheres (Schneider *et al*., 2015; Obrzut *et al*., 2015).

Tubes of 1m long with different diameters (16, 20 and 26 mm), displayed in Fig. 5(a), were employed to characterize the fracture thickness (e_{FR}) influence. To investigate the effects of the fracture outlet initial flow rate (Q_V), the experimental set up was equipped with a globe valve (V-1) positioned at the fracture end, as shown Fig. 5(b). During tests the valve is opened in ¼ turns, i.e., Q_V = 0.25 at each time. Also, to observe the influence of channel flow speed in the fracture filling, different values of the vertical channel Reynolds number (Re), defined in Eq. 1, (150, 300 and 450) were evaluated for the same fracture thickness (e_{FR}), valve opening (Q_V) and particle mass concentration (C_p).

$$\mathrm{Re} = \frac{\rho_g \bar{V} D_H}{\mu_g} \tag{1}$$

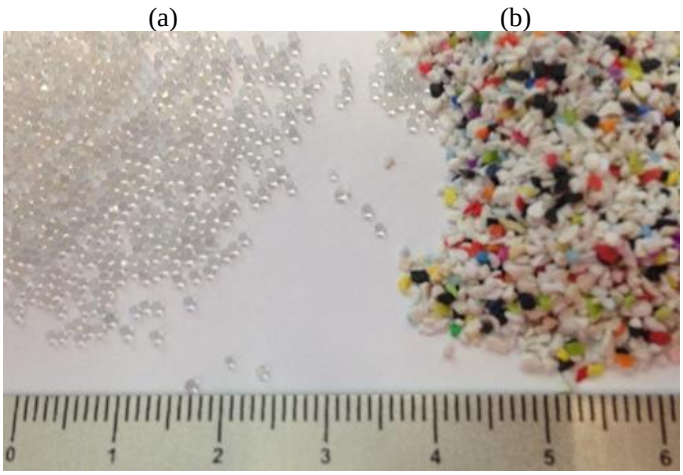

Figure 4. Particulate material employed in the experiments: (a) plastic abrasive (urea) and (b) glass spheres.

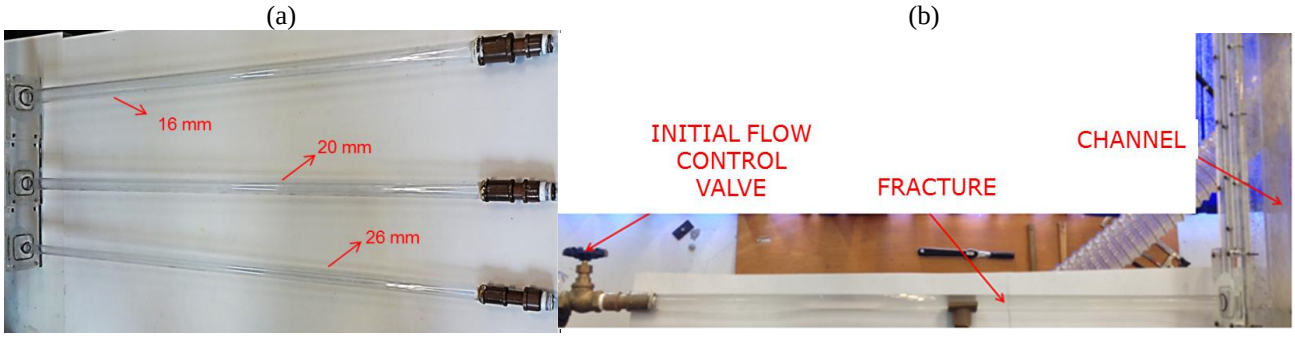

Figure 5. Fracture coupled to test section channel: (a) Tubes representing the fracture (b) fracture overview with fluid flow control valve.

To perform the tests it is necessary to keep the mixing tank (E-2) working for five minutes to homogenize the solution before the screw pump (E-1) be started by a frequency inverter. Thus, the flow starts to pass through the vertical channel as the fracture end valve (V-1) is kept closed. As the homogenized particulate flow is visually verified along the test section, the fracture valve is opened, allowing the fluid to flow at the desired initial flow rate. Measurements and the fracture filming to capture the bed formation are started moments before the opening of the fracture valve.

An electronic board connected to the test section performs the signals acquisition from the meters. The system consists of one chassis and three data acquisition modules responsible for acquiring the signal coming from the equipment. The chassis houses the modules and transmits the signals to a computer. Using a programmed virtual interface, the system acquires the equipment current signals and, from calibration static curves obtained through tests, converts them into flow, pressure and temperature values.

4. RESULTS AND DISCUSSION

In this work the influence of the particle type and concentration, the fracture thickness, flow rate at the fracture end and the Reynolds number on the particle bed formation in the fracture is investigated. Table 1 shows the values adopted for each parameter and the constant parameters for the liquid-solid solution, as well as the tests section geometry in all essay.

The fracture filling process has a deposition rate that decreases in time until the stabilization of the bed is reached. From this moment on particles will no longer enter the fracture and the geometrical parameters, such as the initial position, $h_{p,i}$, extension, h_p , and height, e_p , of the particle bed and also the particles injection time, t_{ip} , as seen in Fig. 6, are determined.

Table 1. Parameters used in all experimental tests.

Mass concentration of glycerin in water	C_g	68.90%
Mass concentration of particulate material in the solution	C_p	2.0 – 2.5 – 3.0%
Particle-fluid density ratio	$\rho_{p/g}$	1.28 – 2.14
Fracture length	h_{FR}	1 m
Channel thickness	h_{CH}	45 mm
Channel depth	Z_{CH}	16 mm
Reynolds number	Re	150 – 300 – 450
Fracture thickness	e_{FR}	16 – 20 – 26 mm
Valve opening for fracture initial flow rate	Q_v	0.25 – 0.5 – 0.75 – 1.0 – 1.25

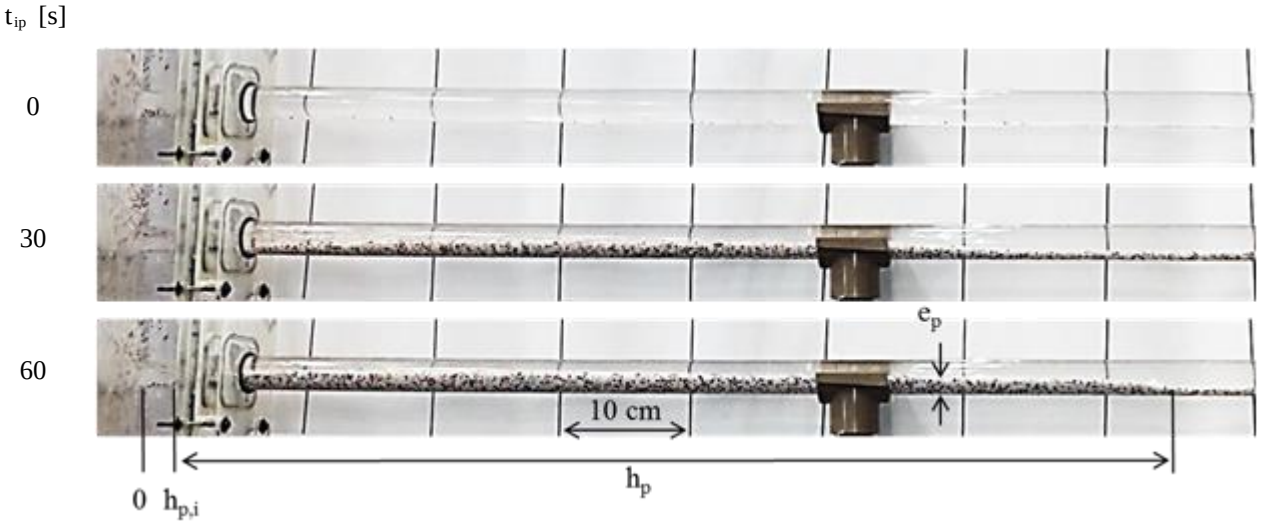

Figure 6. Particle bed geometric parameters over time for e_{FR} =20 mm, Re=150, Q_V =0.75, C_p =3%, $\rho_{p/g}$=1.28.

4.1 Particle injection parameters effect

In this section the variation effect of the particle injection parameters is presented. The particulate material, used to evaluate the fracture filling process, and its concentration are also evaluated.

The granular urea particles ($\rho_{p/g}$ = 1.28) were compared with the glass spheres ($\rho_{p/g}$ = 2.14). The Figure 7 shows the particle bed formed using each material with the same parameters, Re = 300, C_p = 3%, Q_V = 0.75 and e_{FR} = 20 mm.

It's observed that the particle bed formed with the glass spheres presents greater extension (h_p) and height (e_p) in relation to the urea. This occurs due to the higher effective weight of the fluid composed of glass spheres, providing greater particle entry in the fracture.

Figure 7. Particle bed geometric parameters over time for e_{FR} = 20 mm, Re = 300, Q_V = 0.75, C_p = 3%.

Tests to verify the particle concentration effect were performed for a flow with Re = 150, initial fracture flow rate of ¾ valve turn (Q_V = 0.75) and e_{FR} = 20 mm, using urea as particulate material. Three different mass concentration

(C_p) of urea were evaluated (2, 2.5 e 3 %) The Figure 8 shows the final particle bed obtained. The resulting particle bed geometric parameters for these tests are shown in Tab. 2.

The initial positions ($h_{p,i}$) of the three tests are similar, as well as the final time of injection (t_{ip}) in which the particle bed is not modified. However, it is noted that the extension (h_p) and high (e_p) have significant increase as the particle concentration (C_p) increases. The particle concentration increase results in a higher fluid effective weight downstream of the fracture promoting a greater particle entry in the fracture region.

Figure 8. Particle bed geometric parameters over time for e_{FR} = 20 mm, Re = 150, Q_V = 0.75 and $\rho_{p/g}$ = 1.28.

Table 2. Particles bed geometric parameters for different mass concentration of particulate material.

C_P [%]	$h_{p,i}$ [mm]	h_p [mm]	e_p [%]	t_{ip} [s]
2	10	291	35	210
2.5	10	574	60	210
3	10	674	70	210

Figure 9 shows the pressure gradient during time for the tests with the three different mass concentration of particulate material. The pressure gradient is defined as the ratio of the pressure difference measured between the two transducers ($p_{I,2}$ and $p_{I,3}$) and the distance between them (1.54 m), as presented in Eq.(2). It is observed that the pressure gradient has a small increase with the increasing particle concentration.

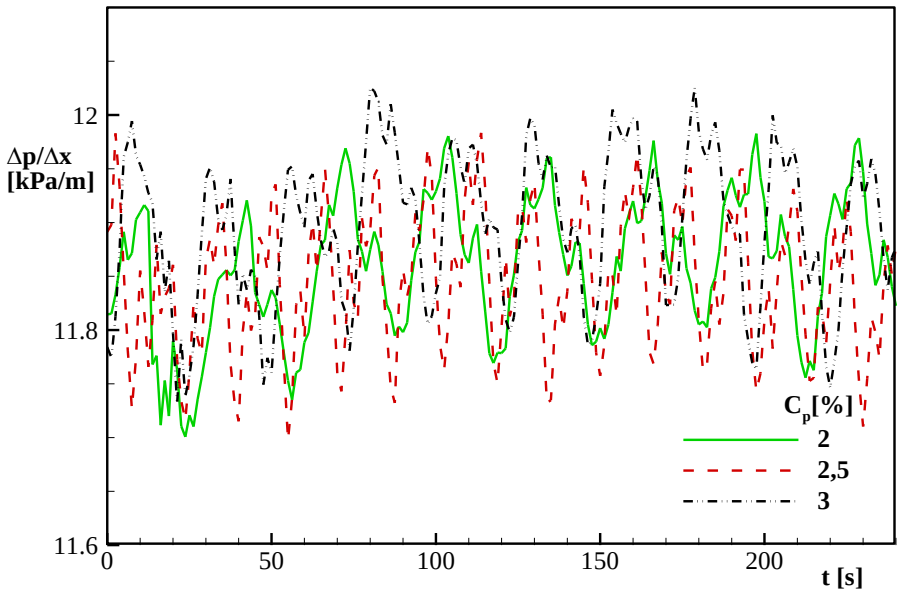

Figure 9. Channel pressure gradient over time for e_{FR} = 20 mm, Re = 150, Q_V = 0.75 and $\rho_{p/g}$ = 1.28.

$$\frac{\Delta p}{\Delta x} = \frac{p_{I,3} - p_{I,2}}{1.54} \qquad (2)$$

4.2 Fluid flow regime effect

In this section the variation effect of the fluid flow regime parameters is presented. The channel Reynolds number and the initial flow rate at the fracture outlet are evaluated as well.

The particle bed obtained for three different Reynolds numbers considering a fracture thickness of e_{FR} = 26 mm, initial fracture flow rate Q_V = 0.5 and C_p = 3% were compared. The Figure 10 shows the stabilized particle beds obtained with Re of 150, 300 and 450. The particles bed geometric parameters for these tests are shown in Tab. 3.

Figure 10. Reynolds number effect over the filling process for e_{FR} = 26 mm, Q_V = 0.5, C_p = 3% and $\rho_{p/g}$ = 1.28.

Table 3. Particles bed geometric parameters for different Reynolds number.

Re	$h_{p,i}$ [mm]	h_p [mm]	e_p [%]	t_{ip} [s]
150	18	176	82	260
300	45	125	40	50
450	60	36	35	40

Tests for different values of Reynolds number in the vertical channel show that as the flow inertia increases with the Re, fewer particles will enter the fracture. Another aspect related to the bed initial position, which significantly increases with increasing Re, is observed due to the high inertia that the particles present within the fracture. In such configurations no particle bed is formed, which represents a total fluid loss through the fracture.

In order to evaluate the fracture initial flow rate influence, the valve positioned at the fracture end was opened in ¼ turns and five different opening levels were compared using the 20 mm fracture thickness (e_{FR}), for Re = 150 and C_p = 3%. Figure 11 shows the final particle bed obtained and its geometric parameters are shown in Tab. 4.

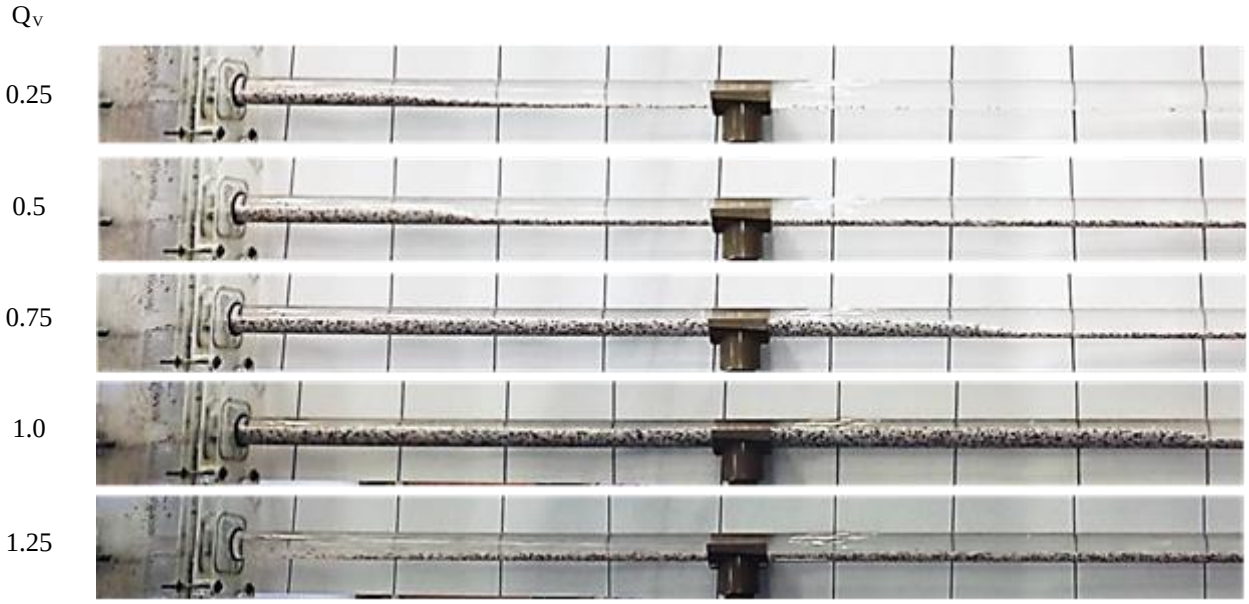

Figure 11. Fracture outlet initial flow rate effect for e_{FR} = 20 mm, Re = 150, C_p = 3% and $\rho_{p/g}$ = 1.28.

Table 4. Particles bed geometric parameters for different initial flow rates.

Q_V	$h_{p,i}$ [mm]	h_p [mm]	e_p [%]	t_{ip} [s]
0.25	27	320	65	105
0.5	25	260	58	120
0.75	25	720	60	165
1.0	27	870	64	350
1.25	-	-	-	-

The results obtained by varying the fracture opening valve (or the initial flow rate), for a constant Reynolds number in a fracture with fixed thickness, show that the higher the flow rate (Q_V) the higher is the length of both the formed bed (h_p) and the filling time (t_{ip}). As the fracture admits a higher flow rate, the velocity at the fracture inlet region is increased, allowing a larger amount of particles to enter the fracture. For a determined valve opening (e.g., Q_V = 1.25) no bed formation is verified.

Figure 12 shows the historic pressure gradient for the different fracture outlet initial flow rate. For the case of Q_V = 1.25 a decrease in the pressure value is observed at $t_{ip} \sim 10$ s, since at this instant the channel outlet pressure is not detected, revealing a severe total fluid loss.

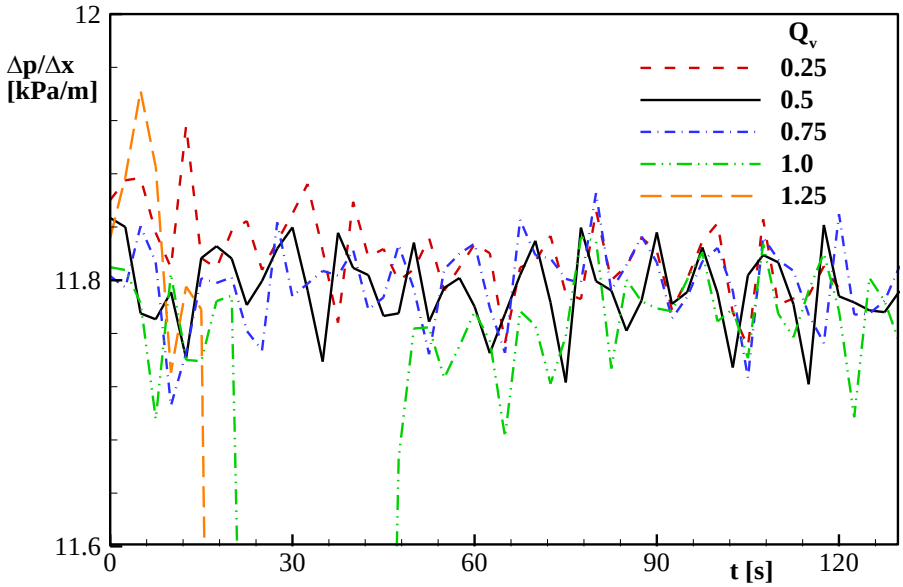

Figure 12. Pressure gradient over time for e_{FR} = 20 mm, Re = 150, C_p =3% and $\rho_{p/g}$ = 1.28.

4.3 Fracture geometric parameters effect

In this section the variation effect of the fracture geometric parameters are presented.

Tests to verify the fracture thickness influence were performed for a flow with Re = 150, initial fracture flow rate of ½ valve turn (Q_V = 0.5) and C_p = 3%, using the three fracture thicknesses (e_{FR} = 16, 20 and 26mm). The Figure 13 shows the final particle beds obtained and related data are shown in Tab. 5.

In general, the tests performed for the three different fracture thickness, for a certain Reynolds number and constant initial fluid flow rate (opening valve), show that the greater the fracture thickness (e_{FR}) the smallest is the length of the particles bed (h_p), but the higher is the bed height (e_p) and the filling time (t_{ip}). The increase in the fracture flow rate area provides a greater number of particles to enter, which, due to the gravity, tends to be deposited closer to the fracture entrance. The Figure 14 shows the pressure gradient during time for the three fracture thicknesses.

Notice that the fracture thickness variation does not exert a significant influence on the pressure gradient along the channel. Over time, each test also shows no variation in the pressure gradient, but an instantaneous decrease occurring close to 10 seconds, is evident as the fracture end valve is opened. This decrease is more pronounced than the characteristic oscillation of the pressure transmitters, which remains around 0.15 kPa/m.

Figure 13. Fracture thickness effect over the filling process for Re = 150 Q_V = 0.5, C_p = 3% and $\rho_{p/g}$ =1.28.

Table 5. Particle bed geometric parameters for different fracture thickness.

e_{FR} [mm]	$h_{p,i}$ [mm]	h_p [mm]	e_p [%]	t_{ip} [s]
16	18	435	50	115
20	22	255	55	120
26	18	176	82	260

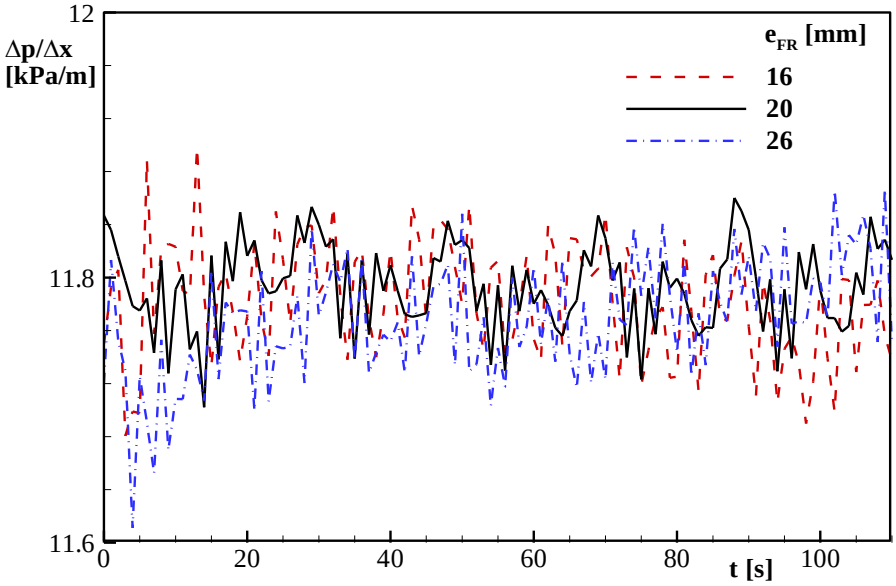

Figure 14. Channel pressure gradient over time for Re = 150, Q_V = 0.5, C_p = 3% and $\rho_{p/g}$ = 1.28.

5. CONCLUSION

In this work, the loss of fluid circulation in a vertical channel due to a transversal fracture is investigated experimentally. The fluid loss is reduced by releasing particulate material in the flow to promote the fracture filling. In general, results show that the particle injection parameters, the fluid flow regime and the fracture geometric parameters are able to modify the geometric characteristics of the bed, having a direct influence on the flow rate, on the amount of particulate material and also on the time required to obtain the final bed. In the particle injection variation tests, a higher effective weight of the fluid, either by increasing the particle concentration or using a solution composed of glass spheres, results in a greater particle entry in the fracture region. For the Reynolds number variation, it was verified that smaller values provides a larger amount of particles to enter the fracture, resulting in better filling formats. As the Reynolds number increases the flow inertia on the fracture region entrance becomes higher, hindering the entry of the particulate material in the fracture. It has been observed that the higher the initial fracture flow rate, the longer the formed bed and the filling time. The increase in the initial fracture flow rate results in a higher velocity in the fracture inlet region, allowing a larger amount of particles to enter the fracture and a larger particle bed. For a given valve

opening a total fluid loss by the fracture occurs, impeding the flow circulation through the channel outlet. Such severe losses, related to the high velocities in the fracture, increase the flow inertia, being able to carry the particles, avoiding the bed formation. In the fracture thickness variation tests, the increase of the flow area by the fracture elevates the number of particles to enter. This happens due to gravity and the particles tend to settle closer to the channel inlet, resulting in higher and less extended beds.

6. ACKNOWLEDGEMENTS

The authors recognize the support of IRF/CENPES/PETROBRAS, the PRH-ANP/MCT program (PRH10-UTFPR) and the National Council for Scientific and Technological Development (CNPq).

7. REFERENCES

Almagro, S.P.B.; Frates, C.; Garand, J.; Meyer A., 2014. “Sealing Fractures: Advances in Lost Circulation Control Treatments”. *Oilfield Review*, v. 26, n. 3, p. 4–13.

Azar, J.J.; Samuel, G.R., 2007. *Drilling Engineering*. Tulsa: PennWell Corporation.

Barbosa, M.V.; De Lai, F.C.; Junqueira, S.L.M., 2016. “Numerical analysis of particulate flow applied to fluid loss control in fractured channels”. In: *Heat Transfer, Fluids Engineering, & Nanochannels, Microchannels and Minichannels Conference*, Washington, DC, ASME HTFEICNMM2016-1028.

Calçada, L.A.; Duqueneto, O.A.; Magalhães, S.C.; Scheid, C.M.; Borges Filho, M.N.; Waldmann, A.T.A., 2015. “Evaluation of suspension flow and particulate materials for control of fluid losses in drilling operation”. *J. Pet. Sci. Eng*., v. 131, p. 1–10.

Cook, J.; Growcock, F.; Guo, G.; Hodder, M.; Van Oort, E., 2012. “Stabilizing the Wellbore to Prevent Lost Circulation”. *Oilfield Review*, v. 23, n. 4, p. 26–35.

De Lai, F.C.; Barbosa, M.V.; Franco, A.T.; Junqueira, S.L.M., 2015. “Eulerian-Lagrangian simulation of particulate flow for sealing fractured channels”. In: *III Multiphase Flow Journeys*, Campinas, SP.

Kumar, A.; Savari, S., 2011. “Lost circulation control and wellbore strengthening: looking beyond particle size distribution”. In: *AADE National Technical Conference and Exhibition*, Houston.

Obrzut, L.Q., De Lai, F.C., Waldmann, A.T.A., Martins, A.L Junqueira, S.L.M., 2015. “Análise experimental de escoamento particulado para o controle de fuga de fluido em canal fraturado”. In *VI Encontro Nacional de Hidráulica de Poços de Petróleo e Gás*, Rio Quente – Goiás.

Schneider, C.L; De Lai, F.C., Junqueira, S.L.M., 2017. “Experimental study of liquid-solid flow applied to lost circulation control in fractured channel”. In *IV Multiphase Flow Journeys*, São Paulo, SP.

Schneider, C.L., De Lai, F.C., Waldmann, A.T.A., Martins, A.L Junqueira, S.L.M., 2015. “Estudo experimental do preenchimento de fraturas com escoamento particulado em canal fraturado”. In *VI Encontro Nacional de Hidráulica de Poços de Petróleo e Gás*, Rio Quente – Goiás.

Suyan, K.M.; Banerjee, S.; Dasgupta, D., 2007. “Practical approach for preventing lost circulation while drilling. Society of Petroleum Engineers”, *SPE* 105251.

Whitfill, D.L.; Hemphill, T., 2004. “Pre-treating fluids with lost circulation materials”. *Drilling Contractor*.

8. RESPONSIBILITY NOTICE

The authors are the only responsible for the printed material included in this paper.